Modelling the interplay between covalent and physical interactions in cyclodextrin-based hydrogel: Effect of water confinement

ARTICLE *in* SOFT MATTER · JULY 2013

Impact Factor: 4.03 · DOI: 10.1039/C3SM50827G

Soft Matter

RSC Publishing

PAPER

Modelling the interplay between covalent and physical interactions in cyclodextrin-based hydrogel: effect of water confinement

Cite this: *Soft Matter*, 2013, **9**, 6457

Vincenza Crupi,[a] Domenico Majolino,[a] Andrea Mele,*[b] Barbara Rossi,*[cd] Francesco Trotta[e] and Valentina Venuti[a]

The vibrational dynamics of a new class of cyclodextrin-based hydrogel is explored in depth here with the aim to clarify the intimate relationship between the structural and functional properties of these innovative polymeric materials. The thorough quantitative analysis of the FTIR-ATR and Raman spectra of the hydrogel obtained by swelling of cross-linked polymers of cyclodextrins with heavy water is performed in the wavenumber range between 1600 and 1800 cm^{-1} by using best-fitting and deconvolution procedures. The use of D_2O instead of H_2O allowed us to separately examine in the vibrational spectra of the hydrogel the C═O stretching bands assigned to the polymer network and the bending mode of engaged water molecules, giving the possibility to explore the structural changes occurring in the polymer network during the hydration process. The experimental findings were interpreted in the light of a comprehensive model which attempts to understand how physical and covalent cross-links combine to determine the macroscopic properties of the gel, like its water holding capacity and the whole rigidity of the gel network. These results shed light on the complex interplay between physical and chemical interactions which yield the formation and stabilization of the hydrogel network, opening the possibility of a rational design of these innovative soft materials for specific technological applications.

Received 22nd March 2013
Accepted 16th May 2013

DOI: 10.1039/c3sm50827g

www.rsc.org/softmatter

Introduction

Over the past years, great effort has been devoted in the physical–chemical research to the development of novel functional systems for effective molecular encapsulation and delivery of active compounds. These materials find important uses for advanced therapeutic methodologies in fast-growing technological fields, like drug delivery, tissue engineering and regenerative medicine.[1–4] Cyclodextrin nanosponges (CDNS) are a very promising class of nanoporous soft materials, capable of encapsulating, carrying and releasing a variety of both lipophilic and hydrophilic compounds,[5–8] including high-molecular-weight molecules (*i.e.* enzymes) by forming with them non-covalent complexes.[9–14]

In particular, β-cyclodextrin nanosponges (β-CDNS) are polymers obtained by polymerization of β-cyclodextrins (β-CD) with cross-linking agents able to react at the free OH of the β-CD units. Some examples are CDNS obtained by using carbonyldiimidazole (CDI),[15–17] pyromellitic anhydride (PMA)[17–19] or ethylenediaminetetraacetic acid dianhydride (EDTAn)[20] as cross-linkers. The final resulting structure is a polymeric network characterized by the simultaneous presence of hydrophobic cavities of β-CD molecules and more hydrophilic channels among the CD units. β-CDNS are solid, insoluble in water and in other common organic solvents and stable at high temperatures[9] up to 300 °C. However, some classes of them can swell in aqueous solutions, giving rise to an interesting gel-like behavior, similar to hydrogel.[18,21,22] Another noticeable advantage of CDNS with respect to common nanoparticles, is represented by the fact that they can be easily regenerated by using different treatments, for example by washing with eco-compatible solvents, by stripping with moderately inert hot gases, by mild heating, or by changing pH or ionic strength.[8] Due to these unique properties, CDNS have been exploited in a variety of technological fields, including agriculture,[12] environmental control,[23] cosmetic and pharmaceutical fields.[14,24–27] In this latter case, it is worth noting the use of CDNS as vehicles for antitumoral drugs such as paclitaxel, camptothecin and

[a]*Dipartimento di Fisica e di Scienze della Terra, Università di Messina, Viale Ferdinando Stagno D'Alcontres 31, 98166 Messina, Italy*

[b]*Department of Chemistry, Materials and Chemical Engineering "G. Natta", Politecnico di Milano, Piazza Leonardo da Vinci 32, 20133, Milano, Italy. E-mail: andrea.mele@polimi.it; Fax: +39 0223993180; Tel: +39 0223993006*

[c]*Dipartimento di Informatica, Università di Verona, Strada le Grazie 15, 37134, Verona, Italy*

[d]*Dipartimento di Fisica, Università di Trento, via Sommarive 14, 38123 Povo, Trento, Italy. E-mail: rossi@science.unitn.it; Fax: +390 461281690; Tel: +390 461282940*

[e]*Dipartimento di Chimica, Università di Torino, Via Pietro Giuria, 10125 Torino, Italy*

tamoxifen.[10,28] Finally, CDNS gels have been used as a chiral reaction environment for photochemical asymmetric synthesis with noticeable capability of asymmetric induction.[29,30]

In spite of these promising applications, several factors like the random nature of the growing process of the polymer, the presence of a large number of reaction sites on each CD unit, and the nature of the polymerization process yielding a large variety of amorphous systems, hampered a systematic structural and dynamic characterization of CDNS. A multi-technique study has been carried out on different classes of β-CDNS, in the dry state, by the combined use of FT-IR spectroscopy in attenuated total reflectance geometry (FTIR-ATR), Raman and Brillouin scattering experiments and quantum chemical calculations.[16,17,19] The inspection of the vibrational dynamics of the polymers over a broad spectral range allowed us to demonstrate that the degree of covalent cross-linking of the polymeric network and the stiffness of the whole material can be effectively tuned by varying the type of cross-linking agent and the reaction conditions, *i.e.* the relative amount of cross-linking agent with respect to the monomer β-CD[16–21] (cross-linking agent/CD molar ratio). In particular, the existence of a characteristic value of cross-linking agent/CD molar ratio was observed, corresponding to the maximum of the cross-linking and stiffness of the polymers, beyond which the excess of cross-linking agent provides branching of CD units rather than polymerization.[17,20] Finally, the detailed analysis of the high frequency vibrational dynamics of nanosponges revealed a clear dependence of the hydrogen-bonded network involving the OH groups of the polymers on the temperature and on the molar ratio between the cross-linking agent and β-CD.[15,16,19]

In this work, we explore the relationship between the structure of CDNS and their swelling ability, as well as the structural and dynamic properties of the corresponding hydrogel obtained by the hydration of the dry polymers with D_2O. Indeed, the cross-linking and branching density as well as the cross-linking/branching ratio are expected to significantly affect the swelling behavior and the macroscopic properties of the CDNS–hydrogel, *i.e.* the capacity of retaining water and the rigidity of the hydrogel network. As a matter of fact, a recent work[29] showed that pyromellitate-bridged cyclodextrin nanosponges exhibit an interesting effect of the phase transition from sol to gel state upon a gradual increase of concentration from 0.2 to 2000 mg mL^{-1} in water. At first, transparent precipitates were formed at low concentration of CDNS, while at higher contents, the solution became a gel-like di-phasic system containing both liquid and gel phases or "flowing gel", and eventually gave a rigid gel at characteristic critical gelation ratios depending on the type of CDNS. High resolution magic angle spinning nuclear magnetic resonance (HRMAS-NMR) measurements, recently performed on the hydrogel of CDNS, detected "free" and "bound" water molecules in the polymeric gel with different diffusion coefficients.[18] Interestingly, similar behavior was recently observed by using the same technique on polymeric anion-exchange membranes.[31] Additionally, in order to shed light on the swelling properties of CDNS, the vibrational dynamics of water molecules confined in the swollen nanosponges has been preliminarily explored as a function of cross-linking degree of the polymers, level of hydration and temperature.[21] The combined analysis of the spectral features of the HOH bending mode (at ~1640 cm^{-1}) and of the O–H stretching vibration (in the 3000–3800 cm^{-1} range) of water molecules allowed us to obtain a detailed picture of the connectivity pattern of H_2O inside the gel phase. Here, we focus our attention on the understanding of water–polymer interactions and their role in determining the structural, dynamic and functional properties of the CDNS hydrogel through the inspection of FTIR-ATR and Raman spectra in a wide frequency range. The use of D_2O instead of H_2O for hydrating polymers allows us to separately examine the effect of water confinement on two different vibration modes: the stretching vibration of the carbonyl groups belonging to the polymer network and the DOD bending mode of engaged D_2O molecules. This experimental approach is revealed to be a powerful tool to investigate the water–polymer interactions, exploiting the possibility to separate, in CDNS swollen with D_2O, the C=O stretching bands of the polymer and the bending mode of water which are usually overlapped. In this way, we are able to propose a comprehensive model of the covalent and non-covalent interactions involved in the formation and stabilization of the hydrogel network. This information is a key preliminary step to optimize the properties of the CDNS–hydrogel for specific applications in different technological fields.[31,32]

Materials and methods

A Chemicals

Cyclodextrin nanosponges were obtained by following the synthetic procedure already described in the Italian patent with minor modification.[33]

In order to obtain the β-CDPMA1*n* polymers, the reactions of polymerization between β-CD and the cross-linking agent pyromellitic anhydride (PMA) at β-CD : PMA molar ratios of 1 : *n* (with $n = 4, 6, 10$) were conducted by dissolving the reagents in dimethyl sulfoxide (DMSO) containing triethylamine and allowing them to react at room temperature for 3 hours. Once the reaction was over, the obtained solid was broken up with a spatula and washed with acetone in a Soxhlet apparatus for 24 h. The pale yellow solid was finally dried under vacuum.

The corresponding hydrogel of the nanosponges was prepared by adding to the dry samples of β-CDPMA1*n* ($n = 4, 6, 10$) a suitable amount of double-distilled and deionized deuterated water (Sigma) in order to obtain two different levels of hydration $h = 3.3$ and 5, where h is defined as the weight ratio D_2O/β-CDPMA1*n*.

All the gel samples were freshly prepared and used for both FTIR-ATR and Raman measurements.

B FTIR-ATR measurements

FTIR-ATR studies were carried out on a DA8 Fourier transform infrared (FTIR) spectrometer from BOMEM, using a thermoelectrically cooled deuterated triglycene sulphate (DTGS) detector, in combination with a KBr beamsplitter and a Globar

source. For all the investigated samples, measurements were performed in the T-range 250–310 K. The gels were contained in a Golden Gate diamond ATR system, based on the attenuated total reflectance (ATR) technique.[34] The spectra were recorded in the 400–4000 cm^{-1} spectral range. Each spectrum was collected with a resolution of 4 cm^{-1}, and is an average of 100 repetitive scans, hence guaranteeing a good signal-to-noise ratio and high reproducibility. No smoothing was done, and spectroscopic manipulation such as baseline adjustment and normalization were performed using the Spectracalc software package GRAMS (Galactic Industries, Salem, NH, USA). As far as the C=O stretching spectral range (1600–1800 cm^{-1}) is concerned, band decomposition was undertaken using the curve fitting routine provided in the PeakFit 4.0 software package, which enabled the type of fitting function to be selected. The strategy adopted was to use well-defined shape components of Voigt functions with all the parameters allowed to vary upon iteration. The statistical parameters were used as a guide to 'best fit' characterized by $r^2 \approx 0.9999$ for all the investigated systems.

C Raman scattering measurements

Raman spectra were recorded on the gel samples placed in an optical quartz cell, at room temperature and in crossed polarization. All the spectra were carried out in backscattering geometry and collected in a wide wavenumber range between 100 and 3800 cm^{-1}. The exciting radiation at 632.8 nm (He–Ne laser, power at the output ~20 mW) was focused onto the sample with a spot size of about 1 μm^2 through the 80X objective of a microprobe setup (Horiba-Jobin-Yvon, LabRam Aramis). The scattered radiation was analysed and detected through a 46 cm focal length spectrograph using a 1800 grooves/mm grating and a charge-coupled device (CCD) detector. The elastically scattered radiation was filtered by using a narrow-band edge filter. The resolution was about 0.35 cm^{-1} per pixel.

The relative amplitude of the luminescence background observed in the Raman spectra is less than a few percent in all the examined samples. The experimental profiles were corrected for the luminescence background by subtracting an interpolating baseline modeled as a linear function. Band decomposition of C=O stretching profile was undertaken by using two Voigt functions implemented in the fitting routine provided in the PeakFit 4.0 software package.

Results and discussion

In the presence of aqueous solutions, β-CDPMA1*n* nanosponges swell,[18,21] giving rise to hydrogels, *i.e.* a three-dimensional network which has the capacity to entrap a large amount of water within its porous structure.[32,35,36]

Previous spectroscopic investigations on β-CDPMA nanosponges in the dry state[17–19] demonstrated that the reaction of polymerization between β-CD and the cross-linking agent PMA involves the formation of ester groups between adjacent molecules of cyclodextrins (Fig. 1(a)), leading to the covalent cross-linked network schematized in Fig. 1(b). Two simultaneous effects which involve different length scales ranging from the mesoscopic to macroscopic domain can be supposed to lead to the formation of the hydrogel network as a consequence of hydration of polymers.

On the one hand, (i) CDNS can swell because of the progressive penetration of water molecules inside the hydrophilic pores of the polymer and, (ii) at the same time, different CDNS domains can aggregate *via* non-covalent (physical) interactions with each other, thus resulting in a three-dimensional network of interconnected domains extending on the macroscopic length scale (*i.e.* the gel), as summarized in Fig. 1(c).

It is reasonable to assume that the intermolecular interactions, which drive the aggregation of nanosized domains in gel phase, are mainly due to hydrogen bonds. This assumption is consistent with the presence, in the structure of CDNS, of both the hydroxyl (OH) groups of cyclodextrins and the ester and residual free carboxylic (C=O) groups[15,19] of the covalent network. All these functional groups are acting as hydrogen bond acceptor or donor groups.

In turn, these hydrogen bonds are mainly responsible of the different behaviours of the CDNS–hydrogel as a function of temperature (vide ultra).

In Fig. 2(a) and (b), the experimental FTIR-ATR and Raman spectra of the β-CDPMA14 hydrogel are reported at two different levels of hydration h, at $T = 290$ K and in the 1600–1800 cm^{-1} wavenumber range. In this spectral region, where typically the stretching vibration of C=O groups falls, cyclodextrins do not show any interfering vibrational bands, thus the intense signals observed both in the IR and Raman spectra of the hydrogel can be assigned to the carbonyl stretching vibrations of esterified PMA.[19] The spectra were preliminary normalized to the intensity of the bands at ≈1030 and 2917 cm^{-1} for IR and Raman data, respectively, according to a protocol proposed for dry CDNS.[16,19,20] The latter vibrational modes are a reliable internal standard, as they are related to the stretching vibrations of C–O and CH_2 groups of the cyclodextrin units, not directly involved in the reaction of polymerization with PMA. This normalization procedure allows the use of C=O stretching band intensities observed in the spectra of the hydrogel (Fig. 2(a) and (b)) as a quantitative descriptor of the population of C=O groups present in the system.[16,19,20]

It is noteworthy that the quantitative analysis of the C=O stretching vibration proved to be impossible in the hydrogel obtained by the hydration of CDNS with H_2O, since in this latter case, the C=O stretching band, centered at ~1710 cm^{-1}, is almost completely convoluted with the HOH bending mode of engaged H_2O at ~1640 cm^{-1}. As a matter of fact, the severe overlap of these spectral components makes their separation unreliable. Thus, the preparation of hydrogel using D_2O instead of H_2O allows this problem to be overcome, since the DOD bending mode is shifted to ~1210 cm^{-1}.

By inspection of Fig. 2, an overall shift to a higher wavenumber of the band assigned to the carbonyl stretching vibration is observed in the Raman spectrum of the hydrogel with respect to the FTIR-ATR profile. This finding calls to mind what was already observed for the corresponding dry polymers[19] and was widely discussed on the basis of a detailed deconvolution of

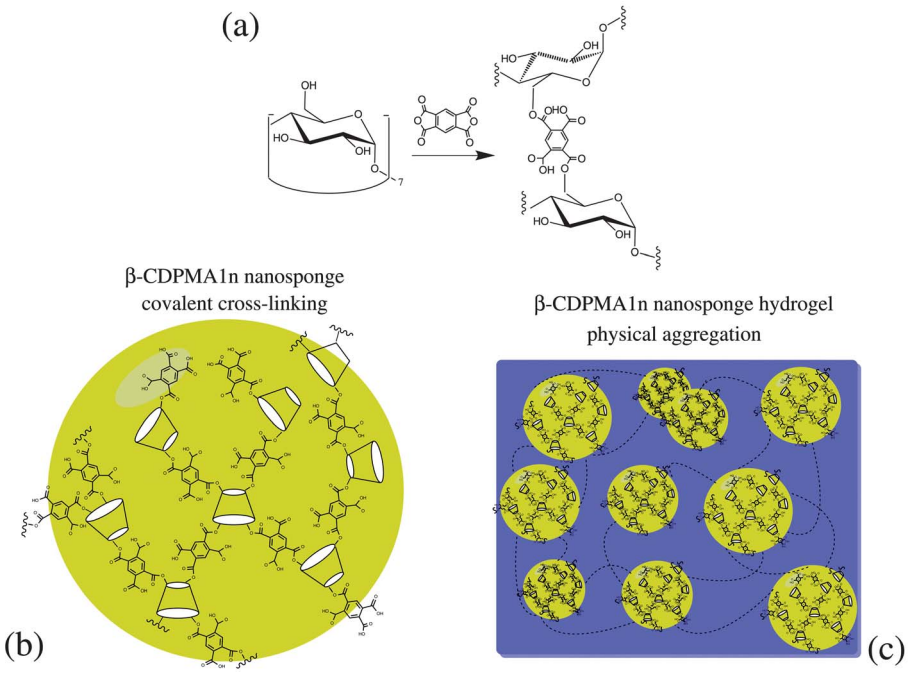

Fig. 1 (a) Scheme of formation of ester groups between two adjacent cyclodextrins. (b) Model of the covalent network of β-CDPMA1*n* nanosponges. (c) Schematic representation of the network of non-covalent interactions among different nanosponge molecules in the gel phase.

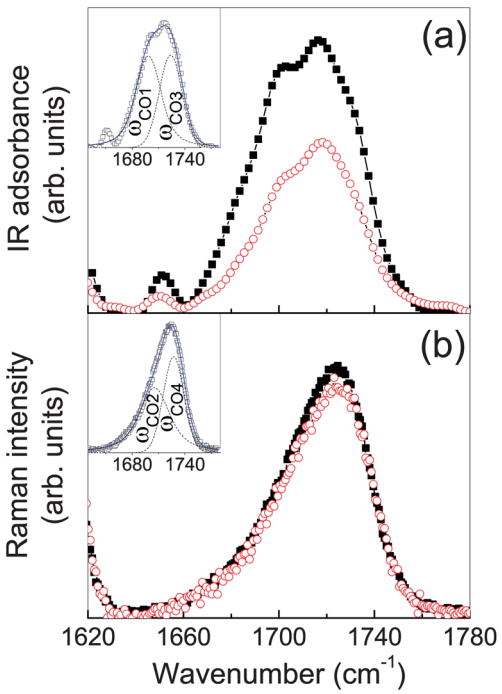

Fig. 2 Experimental FTIR-ATR (a) and Raman (b) spectra in the C=O stretching region of the β-CDPMA14 hydrogel, at $T = 290$ K, as a function of the level of hydration (closed squares: $h = 3.3$, open circles: $h = 5$). Inset: experimental spectra of the β-CDPMA14 hydrogel at $h = 3.3$ together with the best-fit (blue continuous line) and the deconvolution components (dashed lines).

the spectral profile of the C=O stretching band. By following the same approach, four spectral components can be recognized for the C=O stretching band of the hydrogel, *i.e.*, $\omega_{CO1} \cong 1698$ cm^{-1} (IR active), $\omega_{CO2} \cong 1706$ cm^{-1} (Raman active), $\omega_{CO3} \cong 1724$ cm^{-1} (IR active), and $\omega_{CO4} \cong 1728$ cm^{-1} (Raman active). In the insets of Fig. 2(a) and (b), typical examples of the fitting procedure results are reported for IR and Raman spectra of the β-CDPMA14 hydrogel at $h = 3.3$ and $T = 290$ K. The sub-bands ω_{CO1} and ω_{CO2} are ascribed to the stretching vibration of the carbonyl belonging to the ester groups of the esterified PMA, while the sub-bands ω_{CO3} and ω_{CO4} to the C=O stretching vibration of the carboxylic groups of the cross-linker.

The spectra of Fig. 2 show that the total intensity of the C=O stretching band decreases as the hydration level of the hydrogel increases. This effect is more evident in the IR spectrum with respect to the Raman profile. This finding can be explained taking into account that as the water content grows, the molecules of the solvent at the polymer interface tend to saturate the active sites of the nanosponges and, subsequently, to arrange in a more cooperative H-bonded network. As a consequence, the electrostatic environment (in turn related to the first neighbors of the oscillator) experienced by the C=O groups is such that it reduces the overall dipole moment of the CO functional group.

This scenario is consistent with the previously reported FTIR-ATR and Raman analysis of the O–H stretching and HOH bending vibrations of PMA–nanosponge hydrogel in H_2O.[21] On one hand, by increasing the water content, the O–H band showed an increase in the intensity of the low-wavenumber contribution associated with a complementary decrease of the high-wavenumber component, together with an overall low-wavenumber shift of its maximum. On the other hand, a shift towards higher wavenumbers together with an intensity reduction was observed for the HOH bending vibration.

Both these findings indicate an increasing tendency of H_2O molecules to rearrange into highly coordinated H-bond arrangements.

Fig. 3(a) and (b) show the differences between the FTIR-ATR and Raman spectra of the hydrogel obtained by hydration at $h = 5$ of three different types of β-CDPMA1*n* nanosponges ($n = 4$, 6 and 10) in the C=O stretching region. The experimental vibrational profiles recorded on the dry polymers[19] β-CDPMA1*n* are reported in the same spectral range for comparison with the corresponding hydrogel. We remark that previous inelastic light scattering measurements performed on PMA-nanosponges in different frequency regimes[17,19] indicated a clear dependence on *n* of both the covalent cross-linking degree and the whole stiffness (*i.e.* rigidity) of polymers, with a maximum of both parameters observed for a 6-fold excess of cross-linker PMA with respect to the monomer β-CD.

By inspection of Fig. 3(a) and (b), a general shift towards low-wavenumber values of the maximum of the C=O stretching band is observed for the hydrogel with respect to the corresponding dry nanosponges. This occurrence gives evidence that, in the gel phase, the C=O groups of the covalent polymeric network of nanosponges experience a more strongly interconnected H-bonded environment, with a consequent weakening of their dipole moment.[37,38] This experimental evidence strongly supports the validity of the aforementioned model proposed for describing the chemical and physical interactions in the nanosponge hydrogel, *i.e.* the establishment of a network of inter- and intramolecular hydrogen bonds which is superimposed to the covalent cross-linking of polymers. Recent findings on β-CDPMA gels at different water contents by dynamic light scattering are in line with this interpretation.[29]

By comparing the IR spectra of the β-CDPMA1*n* hydrogel, a shift to lower wavenumber of the maximum of the C=O stretching band is observed going from $n = 4$ to $n = 6$, whereas an opposite trend is revealed for $n > 6$. This picture appears more evident in the FTIR-ATR spectra with respect to the Raman profiles, since the carbonyl stretching band is strongly IR-active. The overall shift of the C=O stretching band is reflected by the changes of the centre-frequencies observed for both the spectral contributions to the vibrational band, ω_{CO1} and ω_{CO3}, as indicated in Fig. 4(a).

The components of the C=O stretching mode were isolated from the total experimental profile by using the same fitting and deconvolution procedure described above (see inset of Fig. 3(a) for an example of best-fitting results).

By comparing the evolution as a function of *n* of the frequency positions of the components ω_{CO1} and ω_{CO3} in dry and gel phases (Fig. 4(a)), it appears evident that the hydration of nanosponges leads to the establishment of a hydrogen-bonded network involving the C=O functional groups of the polymers, whose connectivity pattern is strongly dependent on *n*. In particular, we find that the maximum amount of cross-linking observed in dry PMA-nanosponges at a 6-fold excess of PMA with respect to β-CD, is also consistent with the formation of the most strongly interconnected hydrogen-bonded network in the hydrogel, whereas for higher *n* values, the connectivity of the non-covalent cross-links seems to decrease, probably due to the destructuring effects associated with the increased steric hindrance of the polymeric network introduced by the PMA dangling groups.

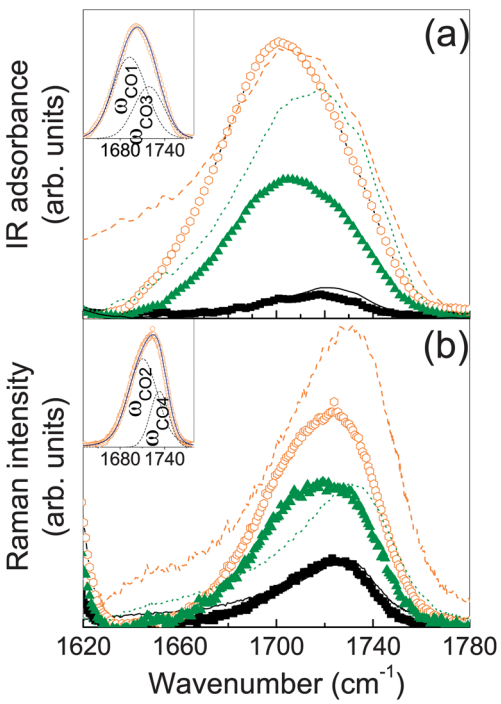

Fig. 3 Experimental FTIR-ATR (a) and Raman (b) spectra in the C=O stretching region of the β-CDPMA1*n* hydrogel (closed squares: $n = 4$, open diamonds: $n = 6$, closed triangles: $n = 10$) at $h = 5$ and $T = 290$ K and of the corresponding dry nanosponges (continuous line: β-CDPMA14, dashed line: β-CDPMA16, dotted line: β-CDPMA110). Inset: experimental spectra of the β-CDPMA16 hydrogel at $h = 5$ and $T = 290$ K together with the best-fit (continuous blue line) and the deconvolution components (dotted lines).

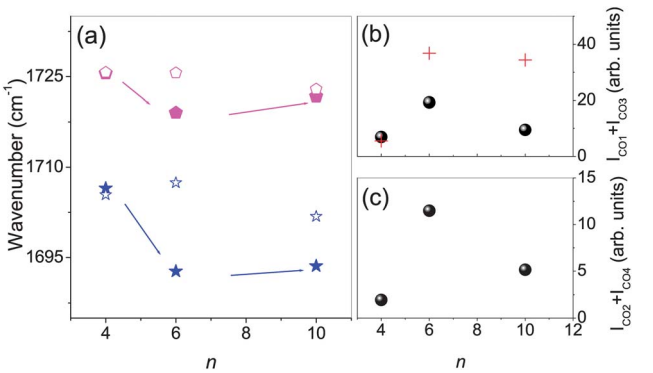

Fig. 4 (a) Frequency-evolution of the spectral contributions to the FTR-ATR C=O stretching band, ω_{CO1} (blue stars) and ω_{CO3} (magenta pentagons) for the β-CDPMA1*n* hydrogel as a function of *n*, at $h = 5$ and $T = 290$ K; open symbols refer to the same components isolated from FTIR-ATR spectra of the corresponding dry β-CDPMA1*n* nanosponges. Total intensity estimated for the C=O stretching band observed in FTIR-ATR (b) and Raman (c) spectra of the β-CDPMA1*n* hydrogel as a function of *n*, for $h = 5$ and $T = 290$ K; red cross symbols refer to the total intensity of the C=O stretching band observed in FTIR-ATR spectra of dry β-CDPMA1*n* nanosponges.

This finding is consistent with the evolution as a function of n of the total estimated intensity of the C═O stretching band, as observed in FTIR-ATR and Raman spectra of the hydrogel and reported in Fig. 4(b) and (c), respectively. The total estimated intensity is obtained as the sum of the intensities of the two different spectral components (I_{CO1} and I_{CO3} for IR and I_{CO2} and I_{CO4} for Raman data) in which the C═O stretching mode has been deconvoluted by using the fitting procedure. The normalized intensity of the C═O stretching band is related to the population of the corresponding functional groups, in turn, directly proportional to the degree of covalent cross-linking in CDNS. The emerging scenario in hydrated CDNS appears to be in agreement with what was already observed for the corresponding dry polymers[17,19] and suggests the finding of the maximum extent of the ester bond formation in the cross-linking reaction of CD with PMA observed at a 6-fold excess of PMA with respect to β-CD. For $n = 6$, the saturation of all the reactive sites of CD is likely to occur, probably due to steric hindrance effects.

Above this value, PMA probably provides a branching of cyclodextrin, rather than a further increase of the cross-linking of the whole system. As expected, the confinement of water in the porous structure of nanosponges does not affect the trend of the cross-linking density found for dry polymers. However, the lower intensity $I_{CO1} + I_{CO3}$ observed for the β-CDPMA16 hydrogel with respect to the dry sample (Fig. 4(b)) reflects the general effect of weakening of the dipole moment of the C═O functional groups already discussed above, due to the establishment of a more cooperative H-bonded network involving the C═O groups in the gel phase.

The interplay between the covalent and non-covalent interactions within the structure of nanosponge hydrogel can be further explored by following the evolution, as a function of n, of the percentage intensities of the different spectral components of the C═O stretching band, I_{CO1} and I_{CO3} for FTIR-ATR and I_{CO2} and I_{CO4} for Raman data, respectively (Fig. 5(a) and (b)). These normalized intensities are representative of the population of the two types of oscillators contributing to the C═O stretching mode, *i.e.* the carbonyl belonging to the ester groups (I_{CO1} and I_{CO3}) and the carboxylic groups (I_{CO2} and I_{CO4}) of the polymer network.

As general result, we find that the trend observed for the percentage intensities I_{COi} as a function of n tends to reproduce the one already revealed for the corresponding dry nanosponges (Fig. 5(a) and (b)), confirming that the excess of ester bonds with respect to the free carboxylic groups is maximum for $n = 6$. This experimental finding confirms, as expected, that the swelling of nanosponges does not affect the populations of the two types of oscillators involved in the C═O stretching vibration. However, even if the general trend turned out to be the same, a different value of the ratio I_{CO1}/I_{CO3} and I_{CO2}/I_{CO4} is observed at the saturation point $n = 6$ by comparing the behaviour of the subbands in the dry state and the gel phase (Fig. 5(c) and (d)). This occurrence reflects the changes in the dipole moment and Raman activity of the spectral components of the C═O stretching band. It can be explained on the basis of the different capabilities of the carboxylic groups to accept hydrogen bonds with respect to the ester groups which, consequently, leads to a different involvement in the H-bonded network of the hydrogel of the two types of carbonyl groups.

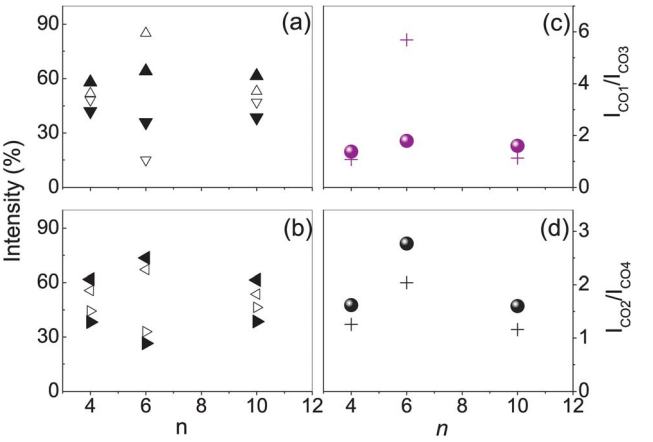

Fig. 5 Percentage intensities of the different spectral contributions to the C═O stretching band as observed in the FTIR-ATR (a) and Raman (b) spectra of the β-CDPMA1*n* hydrogel as a function of n, at $h = 5$ and $T = 290$ K. I_{CO1}: closed up triangles; I_{CO2}: closed left triangles; I_{CO3}: closed down triangles; I_{CO4}: closed right triangles. Open symbols refer to the FTIR-ATR and Raman results obtained on the corresponding dry nanosponges. Ratio between the intensity of the spectral contributions to the C═O stretching band observed in FTIR-ATR (c) and Raman (d) spectra as a function of n; cross symbols refer to the same ratios obtained on the corresponding dry nanosponges.

Fig. 6(a) and (c) indicate the differences in the behaviour of the PMA–nanosponge hydrogel as a function of temperature in the explored range between 250 and 310 K. All the spectra were

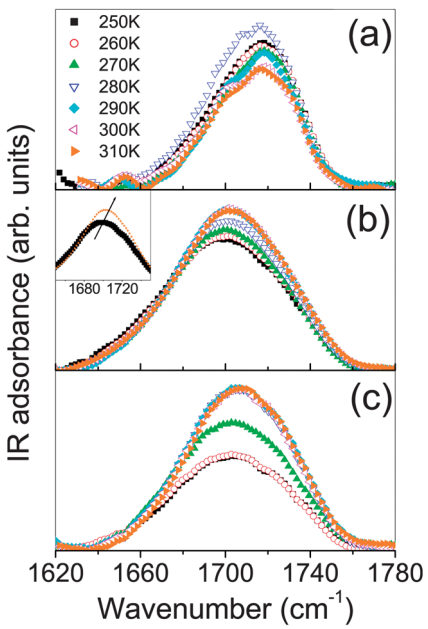

Fig. 6 Experimental FTIR-ATR spectra in the C═O stretching region for β-CDPMA14 (a), β-CDPMA16 (b) and β-CDPMA110 (c) hydrogels, at $h = 5$, as a function of temperature (closed squares: $T = 250$ K, open circles: $T = 260$ K, closed up triangles: $T = 270$ K, open down triangles: $T = 280$ K, closed diamonds: $T = 290$ K, open left triangles: $T = 300$ K, closed right triangles: $T = 310$ K). Inset: comparison between the FTIR-ATR spectra of the β-CDPMA16 hydrogel at $T = 250$ and 310 K.

preliminarily normalized to the intensity of the band at $\approx$1030 cm^{-1}, assumed as a reliable internal standard. For all the investigated hydrogels, a slight shift to a higher wavenumber of the C═O stretching band is revealed by increasing the temperature (see inset of Fig. 6(b)). This finding, in agreement with the behaviour already observed in the same systems hydrated with H_2O,[21] can be explained by taking into account that the thermal motion tends to induce a destructuring effect on the hydrogen-bonded network of D_2O molecules which surround the C═O groups of the polymers.

The deconvolution procedure described above was also applied to the C═O stretching band observed in the FTIR-ATR spectra of the investigated hydrogel at different values of temperature. In Fig. 7, typical examples of best-fitting results for β-CDPMA14 and β-CDPMA110 hydrogels at $h = 5$ are shown for three different values of temperature: the experimental data (open squares) are reported together with the total best-fit (blue continuous line) and deconvolution components (dashed lines) for all the considered profiles. The purpose of this analysis was probing the nature and the extent of changes in the hydrogen-bonded network of the gel phase as a function of temperature. The percentage intensities I_{CO1} and I_{CO3} of the two different IR-active contributions to the C═O stretching band are reported as a function of temperature in Fig. 8(a)–(c) for β-CDPMA14, β-CDPMA16 and β-CDPMA110 hydrogels, respectively. The trends of Fig. 8 give evidence of a temperature-induced destructuring effect on the hydrogen-bonded network of the nanosponge hydrogel, resulting in the variation of the dipole moment of the C═O oscillators observed in the explored temperature range. Interestingly, the different behaviours observed for I_{CO1} and I_{CO3} as a function of temperature (see panels at the right in Fig. 8) reflect a different influence of the thermal motion on the H-bond pattern surrounding the two different types of carbonyl present in the polymer. This fact can be explained, as already suggested above, on the basis of the different capabilities of the carboxylic groups to accept hydrogen bonds with respect to the ester groups, due to the different electron-density distributions on the two types of carbonyls. This finding confirms the suggestion of the existence in the gel phase of two different hydrogen-bond dynamics which involve, on one hand, the ester C═O groups of nanosponges and, on the other hand, the carboxylic groups of the polymer.

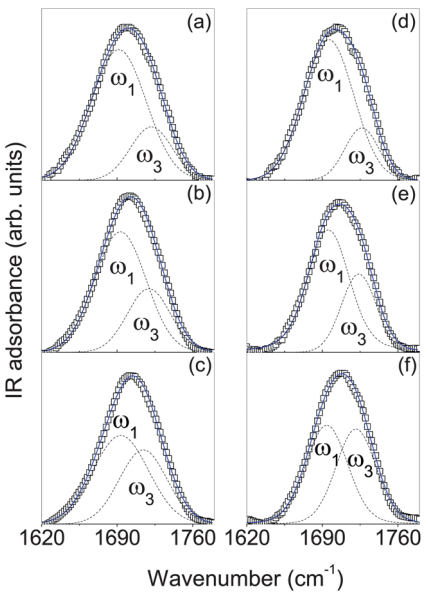

Fig. 7 Typical examples of best-fitting results for the C═O stretching band of the β-CDPMA14 hydrogel at $T = 250$ K (a), $T = 280$ K (b), $T = 310$ K (c) and of the β-CDPMA110 hydrogel at $T = 250$ K (d), $T = 280$ K (e) and $T = 310$ K (f): experimental data (open squares), total best-fit (blue continuous line) and deconvolution components (dashed lines). For both the samples, the hydration level is $h = 5$.

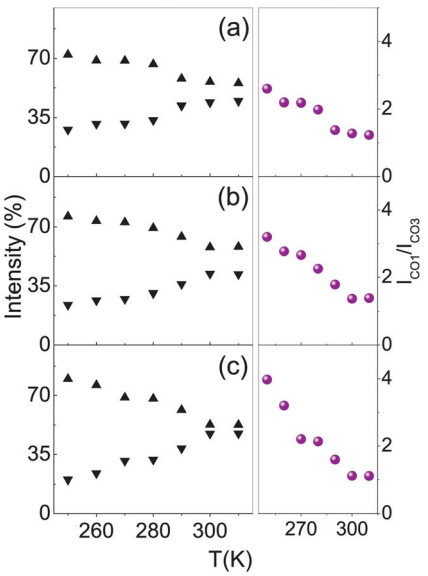

Fig. 8 Temperature evolution of the percentage intensities of the two contributions to the C═O stretching band as observed in the FTIR-ATR spectra of β-CDPMA14 (a), β-CDPMA16 (b) and β-CDPMA110 (c) hydrogels; I_1: up triangles, I_3: down triangles. In the panels at the right, the T-evolution of the corresponding ratios I_{CO1}/I_{CO3} are reported.

Conclusions

A thorough inspection of the vibrational dynamics of an innovative class of cyclodextrin-based hydrogel was carried out here to understand how the interplay between hydrogen-bonded networks and covalent cross-links affects the swelling and macroscopic properties of nanosponges in the gel phase. The hydration of polymers with D_2O instead of H_2O allowed us to follow the effect of water confinement on the spectral features of the vibrational modes assigned to the stretching vibration of the carbonyl groups belonging to the covalent polymer network of nanosponges. To this end, best-fitting and deconvolution procedures were employed for the separation of spectral components contributing to the CO stretching band and for the quantitative analysis of the vibrational spectra. The effect of temperature on the vibrational dynamics of PMA–nanosponge hydrogel was also explored in order to further obtain structural and dynamic information on the system in the gel phase.

A comprehensive model of the physical and chemical interactions established in the gel phase as a consequence of

hydration of CDNS was proposed, in order to interpret the experimental findings. This model suggests that the physical and covalent bonds within the hydrogel combine to determine the macroscopic properties of the gel, like the water holding capacity and the rigidity of the gel network, in a complex interplay. It was found that, on one hand, the aggregation of nano-sized CDNS domains over the macroscopic length scale of the gel is driven by the establishment of inter- and intramolecular hydrogen bonds, and, on the other hand, the rigidity of the polymeric matrix is mainly determined by the covalent cross-linking degree of the polymer. We believe that these results are a key preliminary step to understand the close relationship between the structural and functional properties of the CDNS–hydrogel, also in view of their possible application in many different technological fields.

Acknowledgements

The author B. Rossi acknowledges the financial support of the Regione Veneto, being the beneficiary of a scholarship within the Programma Operativo Regionale FSE 2007–2013.

Notes and references

1 K. Sakurada, F. M. McDonald and F. Shimada, *Angew. Chem., Int. Ed.*, 2008, **47**, 5718.
2 A. Atala, R. P. Lanza, J. A. Thomson and R. M. Nerem, *Principles of regenerative medicine*, Academic Press, Burlington, MA, 2008.
3 F. Van de Manakker, T. Vermonden, C. F. Van Nostrum and W. E. Hennink, *Biomacromolecules*, 2009, **10**, 3157.
4 Y. Tabata, *J. R. Soc. Interface*, 2009, **6**, S311.
5 F. Trotta, W. Tumiatti, R. Cavalli, O. Zerbinati, C. M. Roggero and R. Vallero, Ultrasound-assisted synthesis of cyclodextrin-based nanosponges, Patent number WO 06/002814, 2006.
6 F. Trotta and W. Tumiatti, Cross-linked polymers based on cyclodextrin for removing polluting agents, Patent WO 03/085002, 2003.
7 F. Trotta and R. Cavalli, *Compos. Interfaces*, 2009, **16**, 39.
8 S. Subramanian, A. Singireddy, K. Krishnamoorthy and M. Rajappan, *J. Pharm. Pharm. Sci.*, 2012, **15**, 103.
9 R. Cavalli, F. Trotta and W. Tumiatti, *J. Inclusion Phenom. Macrocyclic Chem.*, 2006, **56**, 209.
10 S. Swaminathan, L. Pastero, L. Serpe, F. Trotta, P. R. Vavia, D. Aquilano, M. Trotta, G. Zara and R. Cavalli, *Eur. J. Pharm. Biopharm.*, 2010, **74**, 193.
11 K. A. Ansari, P. R. Vavia, F. Trotta and R. Cavalli, *AAPS PharmSciTech*, 2011, **12**, 279.
12 L. Seglie, K. Martina, M. Devecchi, C. Roggero, F. Trotta and V. Scariot, *Postharvest Biol. Technol.*, 2011, **59**, 200.
13 R. Allabashi, M. Arkas, G. Hormann and D. Tsiourvas, *Water Res.*, 2007, **41**, 476.
14 F. Trotta, M. Zanetti and R. Cavalli, *Beilstein J. Org. Chem.*, 2012, **8**, 2091.
15 F. Castiglione, V. Crupi, D. Majolino, A. Mele, W. Panzeri, B. Rossi, F. Trotta and V. Venuti, *J. Inclusion Phenom. Macrocyclic Chem.*, 2013, **75**(3), 247.
16 F. Castiglione, V. Crupi, D. Majolino, A. Mele, B. Rossi, F. Trotta and V. Venuti, *J. Phys. Chem. B*, 2012, **116**(43), 13133.
17 B. Rossi, S. Caponi, F. Castiglione, S. Corezzi, A. Fontana, M. Giarola, G. Mariotto, A. Mele, C. Petrillo, F. Trotta and G. Viliani, *J. Phys. Chem. B*, 2012, **116**(17), 5323.
18 A. Mele, F. Castiglione, L. Malpezzi, F. Ganazzoli, G. Raffaini, F. Trotta, B. Rossi, A. Fontana and G. Giunchi, *J. Inclusion Phenom. Macrocyclic Chem.*, 2011, **69**, 403.
19 F. Castiglione, V. Crupi, D. Majolino, A. Mele, B. Rossi, F. Trotta and V. Venuti, *J. Phys. Chem. B*, 2012, **116**(27), 7952.
20 V. Crupi, A. Fontana, M. Giarola, D. Majolino, G. Mariotto, A. Mele, L. Melone, C. Punta, B. Rossi, F. Trotta and V. Venuti, *J. Raman Spectrosc.*, 2013, DOI: 10.1002/jrs.4255.
21 F. Castiglione, V. Crupi, D. Majolino, A. Mele, B. Rossi, F. Trotta and V. Venuti, *J. Raman Spectrosc.*, 2013, DOI: 10.1002/jrs.4282.
22 Y. Takashima, Y. Yuting, M. Otsubo, H. Yamaguchi and A. Harada, *Beilstein J. Org. Chem.*, 2012, **8**, 1594.
23 D. Li and M. Ma, *Clean Products and Processes*, 2000, **2**, 112.
24 P. K. Shende, F. Trotta, R. S. Gaud, K. Deshmukh, R. Cavalli and M. Biasizzo, *J. Inclusion Phenom. Macrocyclic Chem.*, 2012, **74**, 447.
25 R. Cavalli, A. Akhter, A. Bisazza, P. Giustetto, F. Trotta and P. Vavia, *Int. J. Pharm.*, 2010, **402**, 254.
26 A. Vyas, S. Shailendra and S. Swarnlata, *J. Inclusion Phenom. Macrocyclic Chem.*, 2008, **62**, 23.
27 F. Trotta, R. Cavalli, K. Martina, M. Biasizzo, J. Vitillo, S. Bordiga, P. Vavia and J. Ansari, *J. Inclusion Phenom. Macrocyclic Chem.*, 2011, **71**, 189.
28 E. Memisoglu-Bilensoy, I. Vural, A. Bochot, J. M. Renoir, D. Duchene and A. A. Hincal, *J. Controlled Release*, 2005, **104**, 489.
29 W. Liang, C. Yang, D. Zhou, H. Haneoka, M. Nishijima, G. Fukuhara, T. Mori, F. Castiglione, A. Mele, F. Caldera, F. Trotta and Y. Inoue, *Chem. Commun.*, 2013, **49**(34), 3510–3512.
30 W. Liang, C. Yang, M. Nishijima, G. Fukuhara, T. Mori, A. Mele, F. Castiglione, F. Caldera, F. Trotta and Y. Inoue, *Beilstein J. Org. Chem.*, 2012, **8**, 1305.
31 J. E. Jenkins, M. R. Hibbs and T. M. Alam, *ACS Macro Lett.*, 2012, **1**, 910.
32 K. Pal, K. Banthia and K. Majumdar, *Des. Monomers Polym.*, 2009, **12**, 197.
33 F. Trotta, W. Tumiatti and R. Vallero, Italian Patent N. MI2004A000614, 2004.
34 V. Crupi, F. Longo, D. Majolino and V. Venuti, *J. Phys.: Condens. Matter*, 2006, **18**, 3563.
35 R. Langer and D. A. Tirrell, *Nature*, 2004, **428**, 487.
36 A. M. Kloxin, A. K. Kasko, C. N. Salinas and K. S. Anseth, *Science*, 2009, **324**, 59.
37 V. Crupi, D. Majolino, V. Venuti, G. Guella, I. Mancini, B. Rossi, P. Verrocchio, G. Viliani and R. Stancanelli, *J. Phys. Chem. A*, 2010, **114**, 6811.
38 I. Bratu, A. Hernanz, J. M. Gavira and G. H. Bora, *Rom. J. Phys.*, 2005, **50**, 1063.

